

# Experimental Platform for Outdoor Characterization of Photovoltaic Modules Under Hot Climate

Y. M. Soro\*<sup>‡</sup>, Alain K. Tossa\*\*, D. Yamegueu\*, Lionel Sicot\*\*\*

\*LESEE-2iE, Laboratoire Energie Solaire et Economie d'Energie, Institut International d'Ingénierie de l'Eau et de l'Environnement, 01 BP 594 Ouagadougou 01, Burkina Faso.

\*\* KYA-Energy Group, 08BP 81101 Agoenyivé, Lomé, Togo

\*\*\* INES CEA/LITEN- Laboratoire des Modules Photovoltaïques (LMPV), BP 332 –Savoie Technolac, 50 avenue du lac Léman, 73377 Le Bourget-du-lac, France

(moussa.soro@2ie-edu.org, toskalain@gmail.com, Daniel.yamegueu@2ie-edu.org, lionel.sicot@cea.fr)

<sup>‡</sup>Corresponding author: 1 rue de la science, 01 BP 594 Ouagadougou 01 Burkina Faso,

Tel: (+226) 50 49 28 00, Fax: (+226) 50 49 28 01, Email: moussa.soro@2ie-edu.org

*Received: 25.05.2018 Accepted:20.07.2018*

**Abstract** - This paper presents a new test facility for outdoor characterization of photovoltaic modules. The test facility named “I-V bench” has been recently installed, within a sudano - sahelian climate, in Ouagadougou (Burkina Faso). Our principal aim with this bench is to carry out different studies on photovoltaic energy productivity through the characterization of PV modules in real operating conditions. The experimental platform can receive up to 24 modules, from 1 Wp to 600 Wp that can be simultaneously monitored. In this paper, the principle of the operation of the test-bench is described. Then, current and voltage (I-V) data collected with the bench are used to find out the STC values of three different performance settings (open circuit voltage, short circuit current and maximum power) of PV modules. Several methods are proposed in the literature to translate outdoor values into standard conditions ones. Here, a comparison of results obtained with three methods, including the standard NF EN 60891: 1995-02, is performed. It has been shown that although the I-V data translation with model L5P leads to good accuracy, the best results for all photovoltaic parameters are obtained with the standard NF EN 60891: 1995-02. The relative errors obtained with this last method are 1.07 % and 1.13 % for the open circuit voltage and the maximum power respectively.

**Keywords:** Photovoltaic modules, outdoor characterization, standard conditions, I-V curves translation

## 1 Introduction

The principal indicator of a photovoltaic module performance is its current - voltage (I-V) characteristic. The shape of the I-V curve gives information about the quality of the module. The data can be used to determine or extract all the relevant parameters such as the short circuit current  $I_{sc}$ , the open circuit voltage  $V_{oc}$ , the maximum power, the current and the voltage at the maximum power point represented respectively by  $P_{mp}$ ,  $I_{mp}$  and  $V_{mp}$ . Some characteristic parameters of the semiconductor material like the series resistance  $R_s$  and the shunt resistance  $R_{sh}$  can also be deduced from the I-V curves by using numerical models [1, 2].

The photovoltaic module performances given by the manufacturers (in the datasheet) are measured under Standard Test Conditions (STC) defined by an AM 1.5, the junction temperature of 25 °C and a solar radiation of 1000 W/m<sup>2</sup>. Such conditions cannot be met in real outdoor environment. It is thus clear that these optimistic performances will never be obtained in real operating conditions. Indeed, the output parameters of a given PV power plant will be strongly influenced by the climatic and environmental conditions especially the ambient temperature and the solar radiation (solar power and its spectrum) [1, 3, 4]. Furthermore, the impact of these conditions on the PV power plant performances depends on the PV module technology and its manufacturing process [5, 6]. As a consequence, the performance of PV modules

under real conditions can be up to 30% (on a monthly scale) lower than the performance obtained under STC, depending on the weather and the module/cell design [7]. It is therefore essential to know, for a given site, the technology that provides the best tradeoff between the cost and the real performance of the PV module.

For this purpose, this paper presents an outdoor test “I-V bench” installed on the experimental platform of our laboratory (12° 26' 48" North, 1° 33' 45" West) nearby Ouagadougou (capital of Burkina Faso). The test facility is entirely dedicated to the outdoor characterization and the monitoring of the PV modules’ performances. In parallel, the measurements of some local weather parameters including the temperature and solar radiation are collected through the platform. Many issues can be addressed with the outdoor characterization I-V bench. One of them is the performances' comparison study of several PV technologies under real conditions in order to determine the most suitable to sahelian environment. In the present paper, in addition to the description of the facility, we study the translation of I-V curves from sahelian real conditions to STC conditions. Indeed, to compare the performances of different PV technologies, it is necessary to measure the photovoltaic parameters in the same conditions (sun radiation and solar cells temperature). The measurement under standard conditions can be rapidly performed if a “flash test” tool is available. Otherwise, the outdoor measures can be translated into STC values [8]. In the present paper, we will compare the results of I-V data translation using different methods and processes. The translation accuracy will be analyzed in order to find out the appropriate method.

In the first part of this paper, the different components of the I-V bench are described. Then, the operating principle of the I-V measurement is presented. Finally, a comparison of three methods that can be used extract the STC values of the three main parameters of the modules from outdoor measurements is performed.

## 2 I-V facility

The I-V bench is an experimental setup composed of PV modules to be characterized, sensors, resistive loads and measuring devices (ammeter, voltmeter etc.). The IV-bench, is composed of two main parts (see figure 1):

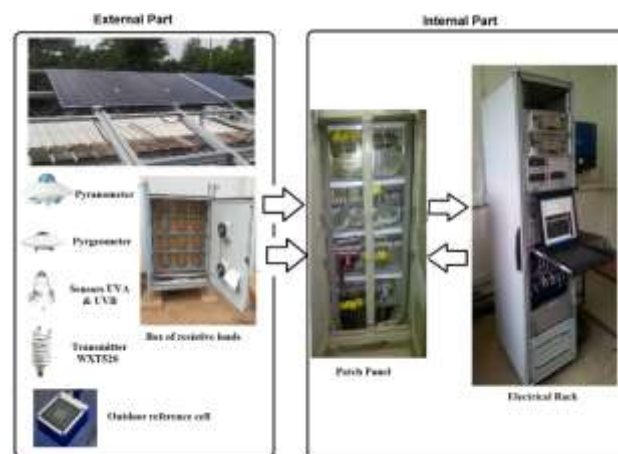


Fig.1. Synoptic view of the I-V bench.

- An external part that can be exposed directly to the sun and in harsh environmental conditions without any bad consequence. This part of the bench can be seen from outside, on the roof of our laboratory building.
- An internal part which is installed inside a room that we called “the characterization room”. It contains sensitive devices such as power supplies, electrical and electronic devices.

These two parts of the bench are described in details in the following sub-sections.

### 2.1 The external part of the bench

The external part of the I-V bench is composed of PV modules’ metal structure, sensors and probes, a box of resistive loads and samples of different PV modules technologies that are to be characterized.

#### – The PV modules metallic structure

The PV modules metallic structure, shown on figure 2, could receive up to 36 PV modules. However, only 24 PV modules can be simultaneously monitored. The 12 additional channels are provided for purpose of reserve or in failures’ case of some of the 24 channels. All different PV module technologies could be tested. The technologies currently under study are: monocrystalline silicon (c-Si), multicrystalline silicon (mc-Si), amorphous (a-Si) and heterojunction silicon (HIT).








Fig.2. Modules metal structure. The inset picture shows the radiation measurement sensors mounted on a plateau that is tilted at the same angle as the modules.

– *The sensors and probes*

As shown on figure 2 (insert picture), five types of sensors are installed on the modules metal structure. A pyranometer, a pyrgeometer and an UV sensor are used to respectively measure the global solar radiation, the infrared fraction and the UV fraction of the sun spectrum. These three devices are installed in the plane of the tilted surface in order to be sure that the real radiation received by the PV modules is measured. A weather transmitter that measures a set of parameters, such as wind speed and direction, the relative humidity and ambient temperature,

is installed close to the modules. The temperature probes (PT 100) are stuck at the rear side of the modules in order to measure the instantaneous module back surface temperature. The temperature of solar cells’ junction is around 3°C greater than the module back surface temperature [9]. Table 1 presents all the five sensors and their functions.

**Table 1.** Sensors for the measurement of meteorological parameters and sun radiation.

Sensors	Function	Picture
Pyranometer	Measurement of solar global radiation on plane or tilted surface. It covers a large spectral range (0.3 - 3µm). No significant spectral selectivity error is expected.	
Pyrgeometer	Measurement of infrared radiation for wavelengths range from 4.5 to ~ 40 µm. It has low temperature dependence sensitivity.	
UV sensors UV-S-AB-T	Measurement of ultraviolet radiation UV-B (282 - 320 nm) and UV-A (320 - 400 nm). Its cosine response is lower than 4 % and the zenith angle is between 0° and 70.	
Reference cell	The reference cell has a response very close to that of modules to be tested. But, as it is smaller and more rapid, it more accurately measures the radiation on tilted surface of the modules with the same technology. Thus, the reference cell leads to a better correlation between the spectral response of the module, the incidence angle of solar radiation and its spectral composition.	
Weather transmitter WXT520	Measurement of six meteorological parameters: wind speed and direction, precipitation, relative humidity, temperature and barometric pressure.	

– *The box of resistive loads*

It is important to note that the characterization of the modules is done one after another. When the characterization of one module is in progress, the 23 other modules must be in open-circuit position or connected to an electrical load. That is the case for the 24 channels when all modules are in “rest state” i.e. they are not being characterized. Since the modules under characterization are generally of different powers, it is not possible to continuously supply their energy to a specific load. In addition, the load should be disconnected every five minutes in order to characterize the module to which it is connected. For all these reasons, it was decided to connect each channel of the bench to a resistive load. Consequently, at a “rest state” the energy of the modules is dissipated in a resistive load. All these resistive loads are installed in a control box called “box of resistive loads” which is also installed outside of the building (see figure 3).



**Fig. 3.** Box of the resistive loads. This box is installed outside to prevent the overheating of the characterization room as we operate under hot climate.

## 2.2 The internal part of the bench

This second part of the bench presented in figure 4, is installed in an air conditioned characterization room for measurement apparatus and electronics safety. This part is composed of an electrical rack that is connected to the external part through a patch panels. The electrical rack includes all the equipment that measure the different parameters needed to analyze the modules' performances. The devices are listed below:

- Three high-precision Agilent multimeters to measure the sun radiation, the PV modules voltage and the photocurrent. The multimeters have 6½ digits and can achieve 10 000 readings a second at 5½-digits. The accuracy for the measurement is about  $\pm 0.03\%$  for DC voltage and  $\pm 0.05\%$  for DC current.
- Four Kepco BOP Bipolar Power Supplies.



**Fig.4.** Internal Part of the I-V bench: (a) Patch panel, (b) Electrical bay.

The Kepco's BOP are fully dissipative, linear stabilizers for laboratory and systems applications [10]. It has two bipolar control channels (voltage or current mode), selectable and individually controllable either from their front panel controls, or by remote signals. In our test facility, the voltage channel is selected and remote-controlled. Kepco's BOP device is also able to operate in all four quadrants of the voltage-current axis. Indeed, their output may swing seamlessly from negative to positive voltages and the output current may also swing from positive to negative values. The result is that, the device acts as a generator or a load, which means it can provide power to a load or absorb electrical power from a power supply. The Kepco BOP device is used in our test facility as a variable impedance which allows the application of various voltages to the terminals of the modules. For each value of voltage, the corresponding current supplied by the module is simultaneously measured by a multimeter. Note that the open-circuit voltage and the short circuit current of the module to be characterized must be in the ranges available on the Kepco BOP device. In fact, every Kepco BOP is defined by the maximum values of voltage and current that it can support without any damage. We have four Kepco BOP devices fairly distributed in two groups. The first group is able to provide a

range of  $\pm 36$  V and  $\pm 12$  A and the range of the second group is  $\pm 100$  V and  $\pm 4$  A. The Kepco belonging to the same group can be connected in series or parallel to enlarge the voltage or current respectively. By this way, the capacity of bench in term of power of module that can be characterized, is also enlarged.

## 2.3 Scientific interests of the I-V test bench

The I-V test bench presented in this paper is able to simultaneously monitor 24 photovoltaic modules regardless of the technology. The nominal power of each module should be in the range of 1 - 600 Wp. Such a test bench with flexible options of monitoring can play a very important role in the PV power plants installation, especially in West Africa region where the lack of metrology systems dedicated to solar energy is crucial. In fact, today all kinds of PV module can be found on African market. Generally, the real origin or manufacturer is unknown and sometime the label on the module can present wrong or inadequate photovoltaic performances.

This test facility aims to determine the real energy production of a given PV module in a given region, regardless of the performances given by the manufacturer [11]. To be more precise, the studies that can be conducted with the I-V bench are listed below:

- The determination of the nominal power of PV modules, and then check the maximum power given by the manufacturer under STC conditions.
- The determination of the energy yield of PV modules from I-V data measured under real operating conditions.
- The development of models (according to PV technologies) that can contribute to a more accurate forecast of the energy production of a given PV power plant in hot environment like Sahelian areas.
- The study of PV modules ageing for different PV technologies. The modeling of the ageing should lead the operator to accurately estimate the life cycle of a PV system in hot environment. Such study could subsequently allow to better design the PV systems and then avoid their under-designing or over-designing.

## 2.4 Operating principle of the bench

The acquisition of the I-V curves can be done by different methods. M. Piliouge et al. [12] have synthesized these methods in five categories. The main difference between these categories lies in the way or the component, used to scan the voltage or the current at the terminals of PV module. Each category is based on one of the following components: variable resistor, capacitive load, electronic load, DC-DC converters and four-quadrant power supply.

Our test facility is based on the four-quadrant power supply category which is also used by several photovoltaic research laboratories [1, 13, 14]. It allows to characterize high power modules since the same types of power supplies can be used to widen the voltage range or the current range when they are connected in series or in parallel respectively. As described below the four-quadrant power supply enables also the capture of the whole I-V curve.



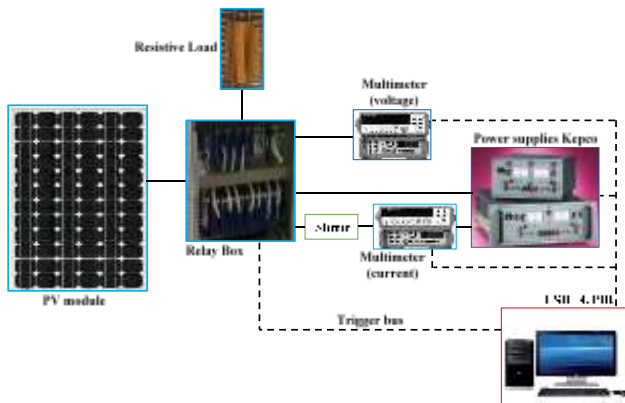


**Fig.5.** Schematic diagram of the I-V curve measurement.

Figure 5 shows the schematic diagram used by the test facility for measuring I-V curve. The acquisition of characteristic data from the bench is done in three steps.

**Step 1: Measurement of the open circuit voltage,  $V_{oc}$**

The screening of the I-V points may be performed from short circuit current ( $I_{sc}$ ) to open circuit voltage ( $V_{oc}$ ) or vice-versa [13] but in both cases such as ours, the module is kept in open circuit before the measurement. Thus, it is preferable to first measure its open circuit voltage. This is done using a digital multimeter (Agilent 34411A) before the characterization of a module.

**Step 2: Choice of the suitable shunt for current measurement**

After the open circuit voltage is measured, a set of shunt resistances are screened via relays in order to select the one which is suitable for the measure of the short-circuit current ( $I_{sc}$ ). The measure of  $I_{sc}$  is done using another digital multimeter (Agilent 34411A).

The values of the current and voltage ( $I_{sc}$  and  $V_{oc}$  respectively) that can be delivered by the module are now determined. The value of  $V_{oc}$  is the highest theoretic voltage that can be applied to the module, in regard of local weather conditions. So normally the power supply should vary the voltage (between the module terminals) from 0 V to  $V_{oc}$ . But in order to capture the whole I-V curve, this interval is slightly modified for the exploration of the points lying in the second and fourth quadrant. This task is possible since the power supply can operate in each of the four quadrants. The bench software allows the setting of the extreme voltages in form of percentages of the measured open circuit voltage.

The desired number of points for the I-V curve plot can also be set (100 points are generally sufficient). Then, the four-quadrant power supply device sets (between the module terminals) several voltages (equal the number of points required for an I-V curve) belonging to the specified interval. Generally, the screening of voltage is done from -0.5 V to 105% of  $V_{oc}$ .

For each point, the multimeters Agilent 34411A simultaneously measure the applied voltage and the corresponding current. Module voltage is measured in a four-wire configuration in order to avoid errors due to voltage drop. The module current is sensed with the help of a shunt resistor

in series between the module and the power supply (see figure 5). The time required for a complete I-V data record is so short (less than 2 s) that the solar radiation can be considered constant for all the points. Nevertheless, some limits are considered in order to avoid the diffusion capacitance effect on the measurements. In fact, as reported in [14–16], the effect known as “diffusion capacitance” influences the I-V curve mainly in the maximum power region; thus, the value of maximum power  $P_{mp}$  can be overestimated or underestimated depending on the speed and direction of the I-V curve screening. Virtuani et al.[16] and Herman et al. [15], show that for high efficiency monocrystalline devices, the capacitive effect strongly starts impacting the I-V curve with screening times lower than 100 ms. In the case of amorphous (a-Si) devices, the capacitive effect impacts the I-V curve only for screening times lower than 10 ms.

**Step 3: "Rest state" of the modules**

Once the characterization is ended, the module is immediately connected to its corresponding resistive load (see figure 3) thank to an appropriated relay. The energy produced by the module is now dissipated in the resistive load and the PV module is said to be in a “rest state”.

The three steps are repeated for all the channels that are connected. The acquisition time of the I-V data when all the 24 channels are connected is less than 1 minute. The interval between two consecutive measures for a same module is set to 5 minutes. In other words, between two measures each module stays in a “rest state” during 5 minutes and it supplies the electricity to the resistive load for the same duration.

In parallel to the I-V curve of each module, several climatic parameters measurements are performed. Thus, for each I-V curve, the solar radiation, the ambient temperature, the cell temperature, the relative humidity, and the wind speed and direction are also available. The measurement devices were chosen to enable acquisitions of I-V curves even at very low irradiance around 0 W/m<sup>2</sup>. The daily measured data are saved in a generic data file (.csv), gathered in one folder which name corresponds to the date of the day. The files contain I-V pairs, estimation of main characteristics of the I-V curves ( $I_{sc}$ ,  $V_{oc}$ ,  $I_{mp}$ ,  $V_{mp}$ ,  $P_{mp}$ , FF etc.), irradiance measurements, temperature, date and time of the measure.

**2.5 Modules installed and characterized**

The first measures of the I-V outdoor test bench presented here have been obtained with three different technologies of silicon photovoltaic modules. The selected modules and their performances under STC conditions are presented in table 2. Since the modules are sorted in class after fabrication, the dispersion in output line can lead to a variation in the performances of the modules belonging to the same class. Thus, the STC characteristics given by the manufacturers cannot exactly represent all the modules having the same reference. Therefore, for a more accurate study, all modules presented here are been characterized under STC conditions with certified set-up in a partner laboratory. The three most important electrical performances of a PV module, generally extracted from the I-V curves are: the maximum power output

$P_{mp}$ , the short circuit current  $I_{sc}$  and the open-circuit voltage  $V_{oc}$ .

The target of this study is firstly to obtain these three performances under STC conditions from the outdoor

measures of the I-V test bench. Then the obtained values will be compared to those measured under STC conditions with a Flashlight Simulator.

**Table 2.** Electrical characteristics (STC) of PV modules installed on the I-V bench.  $N_s$  is the number of cells mounted in series and  $N_p$  the number of strings of solar cells.

PV module	Name of the module	$N_s$	$N_p$	$I_{sc}$ [A]	$V_{oc}$ [V]	$P_{mp}$ [W]
Monocrystalline silicon (Module VSP50M-12V)	VIC001	36	1	3.20	22.50	54.62
Multicristalline silicon (Modules VSP50P-12V)	VIC005	36	1	3.12	21.84	52.23
Amorphous /microcristalline silicon (a-Si:H/ $\mu$ c-Si:H) (Module NA-F128GK)	SHA017	45	4	3.37	61.40	142.47

### 3 I-V Characteristics Translation Methods

The I-V curves are recorded under outdoor weather conditions which, in principle vary continuously. From outdoor I-V curves measurements, it is possible to retrieve the module performances under STC conditions. This task is called the translation of I-V performances [17]. Two processes are commonly used for retrieving the three electrical performances ( $V_{oc}$ ,  $I_{sc}$  and  $P_{mp}$ ) under standard test conditions (STC):

- Process 1: translate all the points of the measured I-V curves under STC conditions before extracting the three electrical performances;
- Process 2: extract firstly the three performances from the measured curves and then translated them to STC in order to retrieve their standard values.

For the two processes described above, the methods basically generally used to translate the I-V curves can be classified in two groups of methods [18]. The first one [2, 19–21] is based on the electrical model parameters ( $I_{ph}$ ,  $R_s$ ,  $R_{sh}$ ,  $I_o$ ,  $n$  ...). The second group of methods [22–25] consists in extrapolating the points of the measured I-V curve directly to STC conditions.

A comparative study performed elsewhere [2] has shown that the five parameters model (L5P) (with an exponential) offers the best trade-off between the computational velocity and the accuracy. Thus, in this study, the first group of the translation methods is considered with the L5P model, and compared to two methods of the second group commonly found in literature [20, 22, 26–29; 30]. The three methods will

be briefly described in the following sub-section.

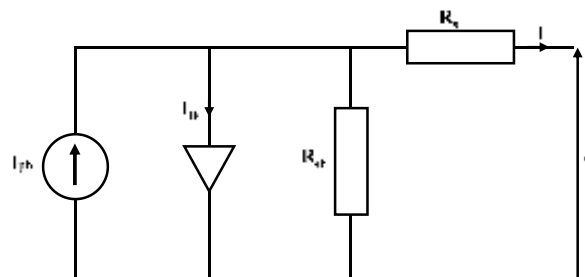


**Fig. 6.** Equivalent electrical diagram of L5P model.

#### 3.1 Method 1: using of L5P electrical model

Figure 6 shows the electrical equivalent circuit of the PV module as well as the parameters to be considered in the modeling. The relation between the electrical parameters is given by the following equation:

$$I = N_p \left( I_{ph} - I_o \left[ \exp \left( \frac{V+I \times R_s}{V_{th}} \right) - 1 \right] - \left( \frac{V+I \times R_s}{R_{sh}} \right) \right) \quad (1)$$

Where

$$V_{th} = \frac{N_s k T}{q} \quad (2)$$

$I_{ph}$  is the photocurrent,  $I_o$  the diode saturation current,  $R_s$  and  $R_{sh}$  the series and shunt resistances respectively,  $N_s$  the number of cells connected in series in each string of the module,  $N_p$  the number of string,  $k$  the Boltzmann constant ( $1.38 \times 10^{-23} \text{ J} \cdot \text{K}^{-1}$ ),  $q$  the electron charge ( $1.6 \times 10^{-19} \text{ C}$ ) and  $T$  the reference cell temperature.

This first method can be performed in two steps to translate the I-V curves measured in outdoor conditions to STC conditions.

*i. Extraction of the electrical parameters*

The five parameters that characterize the LSP method are: the photocurrent ( $I_{ph}$ ), the series resistance ( $R_s$ ), the shunt resistance ( $R_{sh}$ ), the saturation current ( $I_0$ ) and the ideality factor of the diode ( $n$ ). They can be extracted from the measured I-V curve. When one considers the distribution of current-voltage points according to the equation (1), only a numerical method can be effective to determine the parameters with quite accurate values [17]. The approach used in the current study, is based on the Levenberg-Marquardt algorithm (LM) that has been deeply presented in [2]. After obtaining the five parameters, the measured I-V curve can be theoretically reproduced and then translated to any other weather conditions thanks to extrapolation of these parameters to the corresponding weather conditions.

*ii. Extrapolation of the LSP model parameters and obtaining of the I-V curves under STC conditions:*

The following expressions are well suitable for all silicon solar cells technologies [19–21] to extrapolate the LSP model parameters, from one reference weather conditions to any other.

$$I_{ph}(G, T) = I_{ph_{STC}} \left[ 1 + \alpha_{I_{SC}}(T - T_{STC}) \right] \frac{G}{G_{STC}} \quad (3)$$

$$I_0 = I_{0_{STC}} \times \left( \frac{T}{T_{STC}} \right)^3 \times \exp \left( \frac{1}{k} \left( \frac{E_{g_{STC}}}{T_{STC}} - \frac{E_g(T)}{T} \right) \right) \quad (4)$$

$$\frac{E_g(T)}{E_{g_{STC}}} = 1 - 0.0002677(T - T_{STC}) \quad (5)$$

$$\frac{R_s}{R_{s_{STC}}} = \frac{T}{T_{STC}} \left( 1 - \beta \times \ln \frac{G}{G_{STC}} \right) \quad (6)$$

$$R_{sh_{STC}} = R_{sh} \cdot \frac{G}{G_{STC}} \quad (7)$$

The subscript “STC” represents the parameters under STC,  $T$  is the solar cells temperature,  $G$  the solar radiation,  $\alpha_{I_{SC}}$  the temperature coefficient of the short-circuit current (available in the module data sheet),  $E_g$  the semi-conductor material gap in eV and  $\beta$  a coefficient which value is approximately equal to 0.217 [19].

After obtaining the model parameters under STC, the voltage vector under the same conditions must be determined before calculation of the current vector according to equation (1). For the determination of the voltage under STC, we have adopted a process that follows the logic of the I-V curves measurement as described in section 3. The voltage vector,  $V_{STC}$  is determined by following the different steps below:

- $V_{oc,STC}$  is estimated by:

$$V_{oc,STC} = V_{oc} + \alpha_{V_{oc}} \cdot (T_{STC} - T) \quad (8)$$

$\alpha_{V_{oc}}$  is the temperature coefficient of the open circuit voltage (available in the module data sheet);  $T$  and  $T_{STC}$  are the temperature of the module in outdoor conditions and under STC respectively.

- the first value  $V_{STC,1}$  of  $V_{STC}$ , is fixed at - 0.5 V (default value of the bench)
- the last value  $V_{STC,end}$  of  $V_{STC}$ , is fixed at a certain percentage of  $V_{oc,STC}$  previously computed (we will use 105% as it is set for the bench)
- $V_{STC}$  is finally a column vector with the same number of points as the outdoor data voltage vector  $V$  (typically 100), linearly spaced between  $V_{STC,1}$  and  $V_{STC,end}$ .

*3.2 Method 2: extrapolation of the I-V curve from standard NF EN 60891: 1995-02*

As reported by R. Alain [22], A. Ndiaye et al [26], Agroui et al.[31], and according to the standard NF EN 60891: 1995-02, the outdoor measurements under given conditions ( $G, T$ ) are translated into standard test conditions (STC) data by using the following expressions:

$$I_{STC} = I + I_{SC} \left( \frac{G_{STC}}{G} - 1 \right) + \alpha_{I_{SC}}(T - T_{STC}) \quad (9)$$

$$V_{STC} = V + \alpha_{V_{oc}}(T_{STC} - T) - R_s(I_{STC} - I) - K_o I_{STC}(T_{STC} - T) \quad (10)$$

$K_o$ , is the curvature coefficient which takes into account a loss of additional voltage near the maximum power point. For all the modules, a default value  $K_o = 0.002 \Omega / ^\circ C$  is considered, as reported by R. Alain [22];  $\alpha_{V_{oc}}$  is the temperature coefficient of the open circuit voltage (available in the module data sheet).

*3.3 Method 3: extrapolation of the I-V curve from method used in [17, 24]*

Another simple way to translate the I-V curve into STC conditions is obtained by the following expressions [17, 24]:

$$I_{STC} = I \left( \frac{G_{STC}}{G} \right) + \alpha_{I_{SC}}(T - T_{STC}) \quad (11)$$

$$V_{STC} = V + \alpha_{V_{oc}}(T_{STC} - T) - R_s(I_{STC} - I) + V_{th} \ln \left( \frac{G_{STC}}{G} \right) \quad (12)$$

*3.4 Determination of the three electrical performances*

The determination of the three main electrical performances from the measured I-V curves is described as it follows:

- The short circuit current  $I_{sc}$  and the open circuit voltage  $V_{oc}$  are obtained by linear interpolation if the I-V curves intersect the reference axis and by linear extrapolation otherwise.
- The maximum power is obtained by linear interpolation made on the points ( $V, P$ ) where  $P$  is the product of voltage  $V$  and current  $I$ . We consider that  $P_{mp}$  matches the point of the curve ( $V, P$ ) where the gradient  $dP/dV$  is equal to zero. The gradient  $dP/dV$  is estimated by the method of finite differences.

Five cases are considered to determine the standard values of the three parameters ( $I_{sc}$ ,  $V_{oc}$  and  $P_{mp}$ ) of electrical performance by means of the three methods and the two processes:

- **Case 1:** the I-V curve is translated to STC by method 1 before extracting the three parameters (Process 1 by using the method 1)
- **Case 2:** the I-V curve is translated to STC by method 2 and before extracting the three parameters (Process 1 by using the method 2)

- **Case 3:** the I-V curve is translated to STC by method 3 and then extract the three parameters (Process 1 by using the method 3)
- **Case 4:** the parameters from the outdoor I-V curve are extracted first, then each of them is translated to STC by method 2 (Process 2 by using the method 2)
- **Case 5:** the parameters from the outdoor I-V curve are extracted first, then each of them is translated to STC by method 3 (Process 2 by using the method 3)

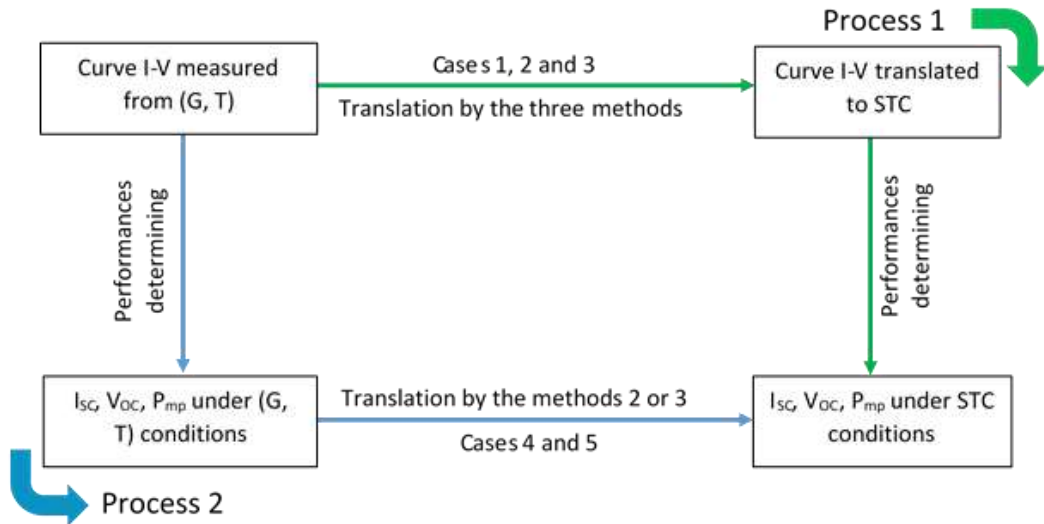


**Fig. 7.** Process of determination of STC values from outdoor measurements. Process 1 (cases 1-3): the whole I-V curve is translated before extracting the parameters ( $V_{oc}$ ,  $I_{sc}$  and  $P_{mp}$ ). Process 2 (cases 4 and 5): the parameters are extracted from outdoor I-V curve before being translated to STC values.

The scheme of figure 7 presents all of the cases considered for the three electrical performances evaluation of this study. Although some studies such as reference [26] limit the translation methods use to specified ranges of irradiance and/or temperatures, the five cases described above are applied here, to all curves measured at irradiance greater than 200  $W/m^2$ . The aim is to determine the case that gives the closest data to those obtained from Flashlight Simulator regardless of weather conditions.

The comparison is performed thanks to the calculation of the relative errors according to the following expressions:

$$\Delta I_{SC} [\%] = \frac{I_{sc_{case;i}} - I_{SC_{Flash\ test}}}{I_{SC_{Flash\ test}}}; \quad i \in \{1,2,3,4,5\} \quad (13)$$

$$\Delta V_{OC} [\%] = \frac{V_{OC_{case;i}} - V_{OC_{Flash\ test}}}{V_{OC_{Flash\ test}}}; \quad i \in \{1,2,3,4,5\} \quad (14)$$

$$\Delta P_{mp} [\%] = \frac{P_{mp_{case;i}} - P_{mp_{Flash\ test}}}{P_{mp_{Flash\ test}}}; \quad i \in \{1,2,3,4,5\} \quad (15)$$

## 4 Results and Discussion

### 4.1 Outdoor experimental data

The Figure 8 presents the trends of the incident radiance  $G$  (measured on the tilted surface of the module) and the module temperature for a clear sky day and a cloudy sky day. A cloudy day is not favorable to a fairly accurate analysis of

outdoor data as the radiation and the temperature strongly vary. For this study, we intentionally chose to analyze the data of the cloudy sky in order to compare the translation methods. Such a situation can be met in the month of August as it is the rainiest period in Burkina Faso, with the lowest sun radiation of the year (but not the lowest temperatures). The modules have been installed on the platform on August 1<sup>st</sup>, 2014 and the results presented here, were collected on August 15<sup>th</sup>, 2014 (15 days after the installation of the modules). The time between their first exposure and the data collection is sufficiently short so that the modules remain clean and unaffected by the ageing phenomena. These precautions are very important to accurately analyze the translation. As a matter of fact, the temperature coefficients provided by the manufacturer should change with the outdoor climatic conditions or ageing phenomena [32, 33].

Despite the fact that the characterization of three PV technologies (see table 2) is ongoing, only one technology (monocrystalline module referenced by VCI001) results will be presented here for sake of clarity. Nevertheless, the results of the other modules lead to the same conclusions.



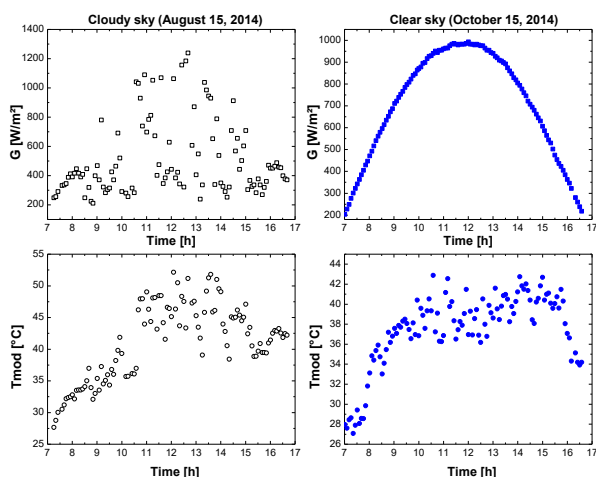


**Fig. 8.** Solar irradiance measurement on the surface of tilted module and the corresponding temperatures of the crystalline module (VIC001) for a cloudy sky (August 15, 2014) and a clear sky (October 15, 2014).

4.2 Comparison of the I-V curves translation methods

We compare the translation of the five methods presented above from the results obtained for three parameters ( $I_{sc}$ ,  $V_{oc}$  and  $P_{mp}$ ).

Table 3 presents for all cases the average values obtained for the three parameters and the corresponding standard deviations.

a) The open circuit voltage translation

The calculation of the  $V_{oc,STC}$  is very sensitive to the translation process with relative errors ranging from 1.07 % to 8.98 % (see figure 9). In fact, the poorest accuracies are achieved when the outdoor  $V_{oc}$  is translated directly to the standard conditions: relative errors of 8.98 % and 8.52 % for cases 4 and 5 respectively. Furthermore, the scattering of the results during the day is so high that the average of  $V_{oc,STC}$  is considerably underestimated. On the contrary, the processes based on translating the whole I-V curve to

standard conditions before extracting the performance parameters give the most accurate results. The best distribution and the lowest error (~ 1 %) are obtained with the case 2, based on the standard NF EN 60891: 1995-02. In sum, it can be noticed that the translation of the open circuit voltage from a given condition to another is very often flawed. Indeed, this parameter depends on intrinsic properties of the material (the ideality factor, the short-circuit current and the saturation current), which in turn are influenced by the sun radiation [9]. This dependence is considered through  $I_{sc}$  in the voltage translation but, it appears to be well considered by methods 1 and 2 through equations (3) and (8) respectively.

**Table 3.** Daily average and standard deviation of the performance parameters calculated under STC ( $V_{oc}$ ,  $I_{sc}$  and  $P_m$ ). They have been estimated for the five processes (Cases 1-5).

	Case 1		Case 2		Case 3		Case 4		Case 5	
Parameters	Avg	Std	Avg	Std	Avg	Std	Avg	Std	Avg	Std
$V_{oc,STC}$ [V]	21.94	0.3129	22.74	0.8121	21.18	0.3847	20.48	0.7315	20.58	0.6775
$I_{sc,STC}$ [A]	3.36	0.3998	3.36	0.4006	3.36	0.4008	3.36	0.4035	3.36	0.4035
$P_{m,STC}$ [Wp]	53.42	7.2228	55.24	7.0921	51.3	6.8779	53.46	6.5171	53.46	6.5171

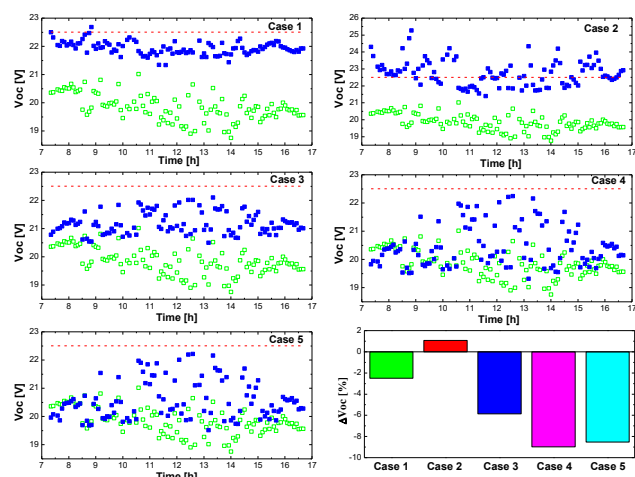


**Fig 9.** Open circuit voltage measurement during the day (full symbol) and the translated values to STC (open symbol) for the five cases. The value measured under STC by mean of the flash test is plotted in red dashed line.

a) The short-circuit current translation

It is well known that the short-circuit current is proportional to the radiation at a same given temperature [9]. Then, any translation error should be related to the accuracy of the temperature coefficient or to a measurement precision. As shown on figure 10, the errors are very close for the five cases (4.63 – 4.83 %) and the distributions are quasi flat. However, in all cases,  $I_{sc,STC}$  is slightly overestimated. It is probably due to the temperature coefficient value provided by manufacturers. In fact, since the manufacturer values of temperature coefficients linked to the modules belonging to the same reference, the dispersions can be noted when considering a specific module. Above all, for the  $I_{sc}$  translation, a classification of the methods is no longer needed; any of the five translation methods can be used.

b) *The maximum power translation*

As the power is the product of voltage and current, the errors in the translation of these last two parameters should influence the accuracy of that of the maximum power. As expected, the lowest relative error and the best distribution are obtained for the case 2 as shown in figure 11. Furthermore, an error of 1.13 % is achieved; this value is very close to that obtained for the open circuit (1.07 %). Whatever the process (see figure 11), the standard NF EN 60891: 1995-02 is the most suitable method for the calculation of the maximum power standard values. This result can be explained by the introduction of the curvature coefficient in equation (10) that considers the loss of power in the vicinity of the maximum power point on the I-V curve. Surprisingly, although the results of the open circuit voltage are relatively poor for the two last cases (cases 4 and 5), the  $P_{mp,STC}$  is well distributed and the accuracy is relatively high. Indeed, for  $P_{mp,STC}$  estimation, the relative error for both cases 4 and 5 is around 1.13 %. The  $V_{oc,STC}$  estimation is 8.97 % and 8.52 % respectively for the two cases. It appears that the good accuracy of the translation of the current offsets the relatively high error of the voltage.

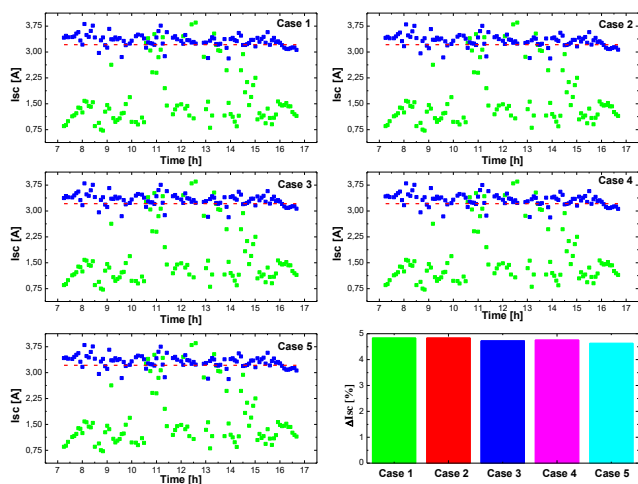


**Fig. 10.** Short-circuit current measurement during the day (full symbol) and the translated values to STC (open symbol) for the five cases. The value measured under STC by means of the flash test is plotted in red dashed line.

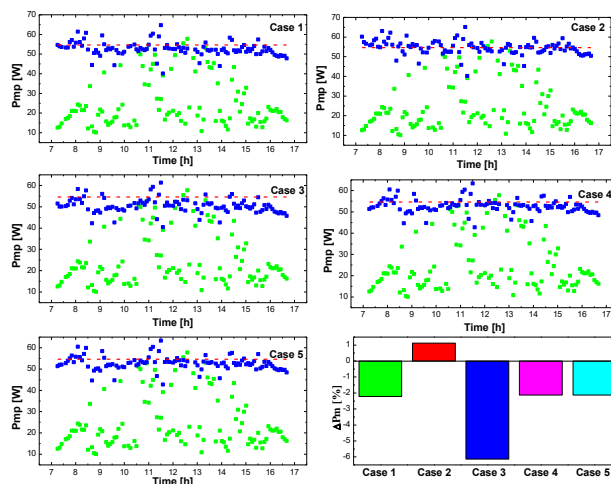


**Fig. 11.** Maximum power measurement during the day (full symbol) and the translated values to STC (open symbol) for the five cases. The value measured under STC by means of the flash test is plotted in red dashed line.

## 5 Conclusion

This paper presents an outdoor characterization tool installed in Ouagadougou (Burkina Faso) for the I-V data measurement in real operating conditions. This I-V test bench is able to monitor simultaneously 24 photovoltaic modules with nominal power from 1 Wp up to 600 Wp. The I-V data are measured in parallel with the solar cells temperature, the sun radiation and weather parameters. Three photovoltaic technologies of silicon (monocrystalline, multicrystalline and amorphous) are currently installed on the platform. The data collection has started since August 2014.

In this study, results of I-V data translation from outdoor conditions to STC for the monocrystalline module are reported. The three translation methods used are based on the L5P model (method 1), the standard NF EN 60891: 1995-02 (method 2) and the model presented by Sadok et al. (method 3). Furthermore, we have adopted two kinds of translation process: translation of the whole I-V data before extracting the photovoltaic parameter (process 1) and direct translation of these parameters (process 2). Several scenarios have been compared through the accuracy of three photovoltaic parameters: the short circuit current, the open circuit voltage and the maximum power. It is shown that the accuracy of a method cannot be effectively judged on the basis of a single parameter. Indeed, the short circuit current is well translated by all the methods with very similar errors range (4.63 - 4.83 %), whereas the translations of open circuit voltage and the maximum power is more accurate with method 2. The relative errors for these two parameters are 1.07 % and 1.13 % respectively. Moreover, it is better to translate all data before extract the performance parameters when considering the large range of irradiance and temperature. The conclusions of this study are a contribution to address the issues of modules' ageing and the impact of the soiling on the productivity of the modules in West Africa climatic zone.

## 6 Acknowledgement:

The I-V bench was funded by European Union through the Flexy-Energy project led by 2iE. Authors would like to thank Laboratory for Photovoltaic Modules (LMPV) of INES-CEA/LITEN for their kind assistance for the construction of the bench.

## References

- [1] J. Merten, L. Sicot, Y. Delesse, and A. G. de Montgareuil, "Outdoor evaluation of the energy production of different module technologies," in *Proceeding of the 23rd European Photovoltaic Solar Energy Conference Exhibition*, 2008, pp. 2841–2845.
- [2] A. K. Tossa, Y. M. Soro, Y. Azoumah, and D. Yamegueu, "A new approach to estimate the performance and energy productivity of photovoltaic modules in real operating conditions," *Sol. Energy*, vol. 110, pp. 543–560, Dec. 2014.
- [3] B. Amrouche, L. Sicot, A. Guessoum, and M. Belhamel, "Experimental analysis of the maximum power point's properties for four photovoltaic modules from different technologies: Monocrystalline and polycrystalline silicon, CIS and CdTe," *Sol. Energy Mater. Sol. Cells*, vol. 118, pp. 124–134, Nov. 2013.
- [4] G. Makrides, B. Zinsser, G. E. Georghiou, M. Schubert, and J. H. Werner, "Temperature behaviour of different photovoltaic systems installed in Cyprus and Germany," *Sol. Energy Mater. Sol. Cells*, vol. 93, no. 6–7, pp. 1095–1099, Jun. 2009.
- [5] A. Hamzeh, S. Hamed, Z. Al-Omari, A. Sandouk, G. Aldahim, "First Year Performance of a PV Plant in Jordan Compared to PV Plants in the Region," *International journal of renewable energy research*, Vol.5, No.4, pp. 983-990, 2015.
- [6] Sara Rodrigues, Mário Baptista Coelho, Pedro Cabral, "Suitability Analysis of Solar Photovoltaic farms: A Portuguese Case Study," *International journal of renewable energy research*, Vol.7, No.1, 2017, pp. 244-254, 2017.
- [7] K. Bücher, "Site dependence of the energy collection of PV modules," *Sol. Energy Mater. Sol. Cells*, vol. 47, no. 1–4, pp. 85–94, Oct. 1997.
- [8] T. Ma, H. Yang, and L. Lu, "Development of a model to simulate the performance characteristics of crystalline silicon photovoltaic modules/strings/arrays," *Sol. Energy*, vol. 100, pp. 31–41, Feb. 2014.
- [9] E. Skoplaki and J. A. Palyvos, "On the temperature dependence of photovoltaic module electrical performance: A review of efficiency/power correlations," *Sol. Energy*, vol. 83, no. 5, pp. 614–624, May 2009.
- [10] "Operator's manual BOP (M) (D) 100W, 200W, 400W Bipolar power supply." Flushing, NY. 11355 U.S.A., 2001.
- [11] Nouar Aoun, Kada Bouchouicha, Rachid Chenni, "Performance Evaluation of a Mono-Crystalline Photovoltaic Module Under Different Weather and Sky Conditions," *International journal of renewable energy research*, Vol.7, No.1, 2017, pp. 293-297, 2017.
- [12] M. Piliougine, J. Carretero, L. Mora-López, and M. Sidrach-de-Cardona, "Experimental system for current-voltage curve measurement of photovoltaic modules under outdoor conditions," *Prog. Photovolt. Res. Appl.*, vol. 19, no. 5, pp. 591–602, Aug. 2011.
- [13] A. J. Bühler, F. Perin Gasparin, and A. Krenzinger, "Post-processing data of measured I–V curves of photovoltaic devices," *Renew. Energy*, vol. 68, pp. 602–610, Aug. 2014.
- [14] G. Friesen and H. A. Ossenbrink, "Capacitance effects in high-efficiency cells," *Sol. Energy Mater. Sol. Cells*, vol. 48, no. 1–4, pp. 77–83, Nov. 1997.
- [15] M. Herman, M. Jankovec, and M. Topič, "Optimal I-V Curve Scan Time of Solar Cells and Modules in Light of Irradiance Level," *Int. J. Photoenergy*, vol. 2012, pp. 1–11, 2012.
- [16] A. Virtuani, H. Müllejans, and E. D. Dunlop, "Comparison of indoor and outdoor performance measurements of recent commercially available solar modules," *Prog. Photovolt. Res. Appl.*, vol. 19, no. 1, pp. 11–20, 2011.
- [17] M. Sadok and A. Mehdaoui, "Outdoor testing of photovoltaic arrays in the Saharan region," *Renew. Energy*, vol. 33, no. 12, pp. 2516–2524, Dec. 2008.
- [18] J. Merten and J. Andreu, "Clear separation of seasonal effects on the performance of amorphous silicon solar modules by outdoor-measurements," *Sol. Energy Mater. Sol. Cells*, vol. 52, no. 1, pp. 11–25, 1998.
- [19] J. Bai, S. Liu, Y. Hao, Z. Zhang, M. Jiang, and Y. Zhang, "Development of a new compound method to extract the five parameters of PV modules," *Energy Convers. Manag.*, vol. 79, pp. 294–303, Mar. 2014.
- [20] A. Luque and S. Hegedus, *Handbook of photovoltaic science and engineering*. Hoboken, NJ: Wiley, 2003.
- [21] F. Attivissimo, F. Adamo, A. Carullo, A. M. L. Lanzolla, F. Spertino, and A. Vallan, "On the performance of the double-diode model in estimating the maximum power point for different photovoltaic technologies," *Measurement*, vol. 46, no. 9, pp. 3549–3559, Nov. 2013.
- [22] A. Ricaud, "Modules et systèmes photovoltaïques." Sep-2008.
- [23] A. Ndiaye, C. M. F. Kébé, P. A. Ndiaye, A. Charki, A. Kobi, and V. Sambou, "A Novel Method for Investigating Photovoltaic Module Degradation," *Energy Procedia*, vol. 36, pp. 1222–1231, Jan. 2013.
- [24] G. Blaesser and E. Rossi, "Extrapolation of outdoor measurements of PV array I–V characteristics to standard test conditions," *Sol. Cells*, vol. 25, no. 2, pp. 91–96, Nov. 1988.
- [25] C. Radue and E. E. van Dyk, "A comparison of degradation in three amorphous silicon PV module technologies," *Sol. Energy Mater. Sol. Cells*, vol. 94, no. 3, pp. 617–622, Mar. 2010.
- [26] C. Rus-Casas, J. D. Aguilar, P. Rodrigo, F. Almonacid, and P. J. Pérez-Higueras, "Classification of methods for annual energy harvesting calculations of photovoltaic generators," *Energy Convers. Manag.*, vol. 78, pp. 527–536, Feb. 2014.
- [27] A. Skoczek, T. Sample, and E. D. Dunlop, "The results of performance measurements of field-aged crystalline silicon photovoltaic modules," *Prog. Photovolt. Res. Appl.*, vol. 17, no. 4, pp. 227–240, Jun. 2009.
- [28] Y. Tsuno, Y. Hishikawa, and K. Kurokawa, "Modeling of the I–V curves of the PV modules using linear

- interpolation/extrapolation,” *Sol. Energy Mater. Sol. Cells*, vol. 93, no. 6–7, pp. 1070–1073, Jun. 2009.
- [29]D. Polverini, G. Tzamalīs, and H. Müllejans, “A validation study of photovoltaic module series resistance determination under various operating conditions according to IEC 60891: Study of photovoltaic module series resistance determination,” *Prog. Photovolt. Res. Appl.*, vol. 20, no. 6, pp. 650–660, Sep. 2012.
- [30]Vanjari Venkata Ramana, Debashisha Jena, D. N. Gaonkar, “An Accurate Modeling of Different Types of Photovoltaic Modules Using Experimental Data,” *International journal of renewable energy research*, Vol.6, No.3, 971 - 974, 2016
- [31]K. Agroui, “Indoor and Outdoor Characterizations of Photovoltaic Module Based on Mulicrystalline Solar Cells,” *Energy Procedia*, vol. 18, pp. 857–866, Jan. 2012.
- [32]T. Ishii, K. Otani, T. Takashima, and S. Kawai, “Estimation of the maximum power temperature coefficients of PV modules at different time scales,” *Sol. Energy Mater. Sol. Cells*, vol. 95, no. 1, pp. 386–389, Jan. 2011.
- [33]P. Kamkird, N. Ketjoy, W. Rakwichian, and S. Sukchai, “Investigation on Temperature Coefficients of Three Types Photovoltaic Module Technologies under Thailand Operating Condition,” *Procedia Eng.*, vol. 32, pp. 376–383, 2012.